DALTON
FULL PAPER

Redox-activated ligand-exchange reactions of tetrabutylammonium *trans*-bis(*tert*-butyl isocyanide)tetrahalogenoruthenate(III) complexes, $[NBu_4][RuX_4(CNBu^t)_2]$ (X = Cl or Br)

Joseph P. al Dulaimi, Robin J. H. Clark * and David G. Humphrey *†

Christopher Ingold Laboratories, University College London, 20 Gordon Street, London, UK WC1H 0AJ

Received 14th October 1999, Accepted 12th January 2000

In situ IR and UV-VIS spectroelectrochemical studies have shown that reduction of the ions *trans*-$[RuX_4(CNBu^t)_2]^-$ (X = Cl or Br) in the presence of acetonitrile or pyridine results in the formation of *mer*,*trans*-$[RuX_3(CNBu^t)_2L]^-$ (L = MeCN or py), which can be oxidised reversibly to *mer*,*trans*-$[RuX_3(CNBu^t)_2L]$. The same reaction carried out in the presence of triphenylphosphine or *tert*-butyl isocyanide yields the disubstituted product, *trans*,*trans*,*trans*-$[RuX_2(CNBu^t)_2L_2]$ (L = PPh_3 or $CNBu^t$), which can be oxidised reversibly in each case to the isostructural monocation. Oxidation of *trans*-$[RuX_4(CNBu^t)_2]^-$ can also be achieved, but the products are dependent upon the identity of the halide. For X = Cl the oxidation is chemically reversible at low temperature forming *trans*-$[RuCl_4(CNBu^t)_2]$, whilst for X = Br the oxidation is irreversible and, in the presence of acetonitrile, pyridine or *tert*-butyl isocyanide, results in the formation of *mer*,*trans*-$[RuBr_3(CNBu^t)_2L]$ (L = MeCN or py) or *mer*-$[RuBr_3(CNBu^t)_3]$ (L = $CNBu^t$). All of the redox products have been characterised *in situ* by IR and UV-VIS spectroscopy in as many oxidation states as possible.

Introduction

Various tervalent ruthenium monoanions of general formula *trans*-$[RuX_4L_2]^-$ are known in which X is halide and L a neutral donor ligand.[1–11] Of particular significance are the chloride complexes in which L is a heterocyclic nitrogen-donor ligand; these complexes have been shown to be effective agents against certain strains of cancer tumour,[12–15] a property which is thought to be linked to their redox chemistry. The reduction of the complex *in vivo* may result in the dissociation of chloride and the co-ordination of the ruthenium-containing moiety to a nitrogen base of DNA.[16,17] In an effort to understand the redox chemistry of this general class of complexes, the ions *trans*-$[RuX_4(CNR)_2]^-$ (X = Cl or Br; R = Bu^t) have been prepared and are the subject of the work described herein.

The complexes *trans*-$[NBu_4][RuX_4(CNBu^t)_2]$ were first prepared as part of a study concerned with the additive (and non-additive) effect of ligands in binary halide–neutral donor ligand complexes.[18] A recent spectroelectrochemical investigation of *trans*-$[NBu_4][RuBr_4(CNBu^t)_2]$ in acetonitrile has indicated that both its oxidation and reduction are accompanied by processes which give rise to new species in solution,[19] *i.e.* its redox chemistry is dominated by EC-type behaviour in which electron transfer (E) is followed by a homogeneous chemical reaction (C). The purpose of this work is to explore the generality of these methods of activation and to extend these studies to the analogous chloride species, *trans*-$[RuCl_4(CNBu^t)_2]^-$. Described herein are the results of detailed electrochemical and spectroelectrochemical studies of *trans*-$[NBu_4][RuX_4(CNBu^t)_2]$ (X = Cl or Br).

The redox chemistry of these complexes is particularly amenable to investigation by *in situ* IR and UV-VIS spectroelectrochemical techniques. The NC stretching vibration (ν_{NC}) of a co-ordinated isocyanide ligand gives rise to a strong absorption band in the 1600–2300 cm^{-1} region of the IR spectrum,[20–25] with ν_{NC} being sensitive both to the bonding mode of the isocyanide and to the oxidation state of the metal. Isocyanide ligands can stabilise transition metal ions in a range of oxidation states, such that the co-ordinated isocyanide ligands may provide a convenient 'handle' with which to follow, by IR spectroscopy, the redox chemistry of complexes of which they are part. Although UV-VIS spectra are frequently not structurally informative, this is not the case for the present system for which the spectra can be particularly instructive in helping to identify redox products, especially those for which the tervalent state is accessible. The UV-VIS spectra of tervalent complexes $[RuX_nL_{6-n}]^z$ (X = halide; L = neutral π-acceptor ligand, $n \geq 2$) are in general dominated by halide(pπ)-to-Ru(dπ) charge-transfer (XMCT) transitions,[26,27] and certain chromophores are often readily identifiable *via* such spectra, *e.g.* *trans*-$[RuX_4L_2]^-$, *mer*-$[RuX_3L_3]$ and *trans*-$[RuX_2L_4]^+$. Within this work, both IR and UV-VIS spectroelectrochemical techniques have been used extensively to characterise the products formed in the redox reactions of the complexes *trans*-$[NBu_4][RuX_4(CNBu^t)_2]$ (X = Cl or Br).

Experimental

Samples

The complexes *trans*-$[NBu_4][RuX_4(CNBu^t)_2]$ (X = Cl or Br) were prepared by modification of the literature procedure and characterised by UV-VIS and IR spectroscopy, fast-atom-bombardment mass spectrometry, and elemental analysis (C, H, N).[18]

Electrochemical measurements

Voltammetric experiments were generally performed as described previously,[28] using a one compartment cell which supported a platinum-bead working electrode, a platinum-coil auxiliary electrode and a Ag–AgCl reference electrode, against which the ferrocenium–ferrocene ($Fc^{+/0}$) couple was measured at +0.55 V. All voltammetric data were uncorrected for *iR* drop. Bulk electrolyses were carried out in a two-compartment cell, with a platinum-basket working electrode and Ag–AgCl reference electrode separated from the platinum auxiliary electrode

† Present address: CSIRO Division of Forestry and Forest Products, Private Bag 10, Clayton South MDC, Victoria 3169, Australia. E-mail: David.Humphrey@ffp.csiro.au

by a double-fritted salt bridge. Solvents and electrolytes were dried and prepared as described previously.[28]

Spectroelectrochemical measurements

The IR spectroelectrochemical experiments were performed using an infrared reflection-absorption spectroscopic (IRRAS) cell,[29] mounted in the sample compartment of a Nicolet 750 FTIR spectrometer on a modified Specac specular reflectance attachment (PN 19.170).[30] The electrode arrangement consisted of a polished platinum-disk working electrode (radius = 2.5 mm), a platinum-basket auxiliary electrode, and a platinum-wire pseudo-reference electrode. In a typical experiment, the background spectrum (single scan, 1.0 cm^{-1} resolution) was collected with the platinum working electrode wound down against the KBr (or CaF_2) window. The desired film thickness was then set (50–100 μm) and an initial spectrum recorded. The working electrode was stepped to an appropriate potential (E_{app}), usually 200 mV past $E_{1/2}$ or E_p for the complex under investigation, and single scan spectra were collected as a function of time. In general, electrolyses were complete within several minutes. Spectra collected in this manner have solvent–electrolyte bands superimposed on those of the sample complex, but these can be subtracted with an Omnic® software routine. An alternative procedure involves collecting sample spectra *versus* a pre-collected solvent–electrolyte spectrum loaded into the background memory. Difference spectra can be calculated by subtracting the initial spectrum from each spectrum in turn. Cooling of the cell was achieved by passing chilled nitrogen gas through the core of the working electrode.[30]

The UV-VIS spectroelectrochemical experiments were performed using an optically transparent thin-layer electrolysis (OTTLE) cell,[31] mounted in the sample compartment of a Perkin-Elmer Lambda 16 spectrophotometer. The cell, a quartz cuvette (pathlength = 1.0 mm), contained a platinum-gauze working electrode which transmitted ≈75% of incident light. The platinum-wire auxiliary and pseudo-reference electrodes were arranged in the top of the cell. A hollow rectangular Teflon block, separated into three sections by quartz windows, was used to hold the cell during an experiment. The OTTLE cell was mounted into the middle section of the block and cooled by a regulated flow of chilled nitrogen gas passing over its faces. Nitrogen gas at ambient temperature was also passed through the outer sections of the block to prevent fogging of the quartz windows. For those complexes that were electrogenerated quantitatively and characterised *in situ* by UV-VIS spectroscopy, molar absorption coefficients (ε) were calculated from the ε values of the starting complexes, *trans*-$[NBu_4][RuX_4(CNBu^t)_2]$ (X = Cl or Br).

Results and discussion

General redox behaviour

The tervalent ions *trans*-$[RuX_4(CNBu^t)_2]^-$ (X = Cl or Br) undergo one-electron oxidation and reduction to yield ruthenium-(IV) and -(II) species respectively. Generally the simple one-electron redox products are not stable on timescales longer than that of the cyclic voltammetric experiment as they undergo homogeneous chemical reactions to yield a variety of products. The chemistry associated with the reduction of these complexes is generally similar for X = Cl or Br, whereas that accompanying oxidation differs significantly depending upon the identity of the halide.

Reduction of *trans*-$[RuX_4(CNBu^t)_2]^-$ in the presence of a neutral ligand L (MeCN or py)

The cyclic voltammogram of an acetonitrile–dichloromethane (1:1) solution of *trans*-$[NBu_4][RuBr_4(CNBu^t)_2]$ containing 0.25 mol dm^{-3} $[NBu_4][PF_6]$ is shown in Fig. 1(a). The complex exhibits an irreversible reduction at $E_{pc} = -0.18$ V, which leads to the formation of another electroactive species which is detected on the return and subsequent scans at $E_{1/2} = +0.41$ V. Bulk reduction at $E_{app} = -0.40$ V consumes 1 F of charge per mol of complex, as does reoxidation at $E_{app} = +0.60$ V. The cyclic voltammogram of the solution after these electrolyses is shown in Fig. 1(b). Spectroelectrochemical studies have indicated that the product of reduction of *trans*-$[RuBr_4(CNBu^t)_2]^-$ in the presence of acetonitrile is *mer*,*trans*-$[RuBr_3(CNBu^t)_2(NCMe)]^-$, which in turn can be oxidised reversibly to *mer*,*trans*-$[RuBr_3(CNBu^t)_2(NCMe)]$.[19] The results of bulk electrosynthesis are in accord with these previous results, such that the waves detected at +0.41 and +1.85 V in Fig. 1(b) correspond to the $Ru^{III/II}$ and $Ru^{IV/III}$ couples of *mer*,*trans*-$[RuBr_3(CNBu^t)_2(NCMe)]$ respectively (Table 1). The irreversible waves observed at +0.95 and +1.26 V in Fig. 1(b) are due to the oxidation of free bromide,[32] which had been expelled from the parent complex upon reduction.

The redox behaviour of the analogous chloride complex is qualitatively very similar. The cyclic voltammogram of *trans*-$[NBu_4][RuCl_4(CNBu^t)_2]$ dissolved in acetonitrile–dichloromethane (1:1) containing 0.25 mol dm^{-3} $[NBu_4][PF_6]$ is shown in Fig. 2(a). The IR spectroelectrochemical studies indicate the formation of *mer*,*trans*-$[RuCl_3(CNBu^t)_2(NCMe)]^-$ upon reduction, *i.e.* the growth of a single ν_{NC} band at 2111 cm^{-1} suggests the retention of two *tert*-butyl isocyanide ligands in a transoid arrangement,‡ whilst the appearance of a weak band at 2272

Table 1 Electrode potentials

Complex (z = charge)	$E_{1/2}$ [a]/V $Ru^{IV/III}$	$Ru^{III/II}$
$[RuCl_4(CNBu^t)_2]^{z}$ [b]	+1.53 (qrev)	−0.28 (rev) [c]
$[RuBr_4(CNBu^t)_2]^{z}$ [b]	+1.46 (irrev) [d]	−0.20 (rev) [c]
$[RuCl_3(CNBu^t)_2(NCMe)]^{z}$ [e]	+2.06 (irrev) [d]	+0.33 (rev) [f]
$[RuBr_3(CNBu^t)_2(NCMe)]^{z}$ [e]	+1.85 (irrev) [d]	+0.41 (rev) [f]
$[RuCl_3(CNBu^t)_2(py)]^{z}$ [e]	—	+0.27 (rev) [g]
$[RuBr_3(CNBu^t)_2(py)]^{z}$ [e]	—	+0.33 (rev) [g]
$[RuCl_3(CNBu^t)_3]^{z}$ [h]	—	+0.65 (irrev) [i]
$[RuBr_3(CNBu^t)_3]^{z}$ [h]	—	+0.68 (irrev) [i]

[a] *vs.* Ag–AgCl, against which ferrocenium–ferrocene is measured at +0.55 V. rev = reversible, qrev = quasi-reversible, irrev = irreversible. [b] *trans* Isomer. [c] Recorded in 0.5 mol dm^{-3} $[NBu_4][PF_6]$–CH_2Cl_2 at 213 K. [d] Irreversible, E_{pa} quoted. [e] *mer*,*trans* Isomer. [f] Recorded in 0.1 mol dm^{-3} $[NBu_4][PF_6]$ in CH_2Cl_2–MeCN (1:1) at ≈233 K. [g] Recorded in 0.5 mol dm^{-3} $[NBu_4][PF_6]$ in CH_2Cl_2–py (1000:1) at ≈290 K. [h] *mer* Isomer. [i] Recorded in 0.5 mol dm^{-3} $[NBu_4][PF_6]$–CH_2Cl_2 containing 5 mol equivalents of $CNBu^t$ at ≈290 K.

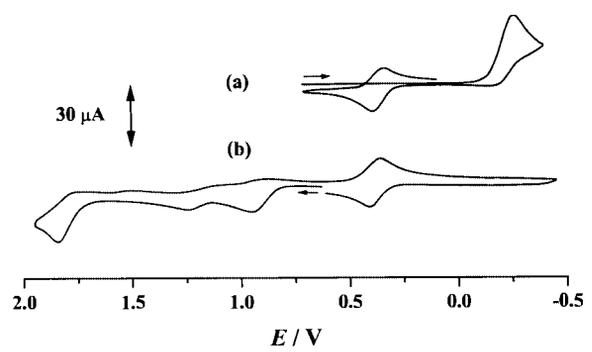

Fig. 1 (a) Cyclic voltammogram of *trans*-$[NBu_4][RuBr_4(CNBu^t)_2]$ in an acetonitrile–dichloromethane (1:1) solution containing 0.25 mol dm^{-3} $[NBu_4][PF_6]$ at ≈290 K. (b) Cyclic voltammogram after consecutive bulk electrolyses at $E_{app} = -0.4$ and +0.6 V respectively. Scan rate = 100 mV s^{-1} in each case.

‡ Under the C_{2v} point group, two ν_{NC} bands (a_1 + b_1) are anticipated; however the dipole moment changes for the a_1 mode will almost cancel out such that one strong band (b_1) and one weak band (a_1) are expected. Deviation from C_{2v} symmetry on account of bending along the Ru–CN–C axis would result in increased intensity of the band attributed to the a_1 mode.

Table 2 IR Data

Complex (z = charge)	Band maximum[a]/cm^{-1} ν_{NC}, Ru^{IV}	ν_{NC}, Ru^{III}	ν_{NC}, Ru^{II}	ν_{CN}
$[RuCl_4(CNBu^t)_2]^{z\,b}$	2240m	2176s	—	—
$[RuBr_4(CNBu^t)_2]^{z\,b}$	—	2170s	—	—
$[RuCl_3(CNBu^t)_2(NCMe)]^{z\,c,d}$	—	2196s	2111s, ≈2070 (sh)	2272w (Ru^{II}), 2328w (Ru^{III})
$[RuBr_3(CNBu^t)_2(NCMe)]^{z\,c,d}$	—	2192s	2109s, ≈2070 (sh)	2275w (Ru^{II}), 2326w (Ru^{III})
$[RuCl_3(CNBu^t)_2(py)]^{z\,c,e}$	—	2189s	2102s,	—
$[RuBr_3(CNBu^t)_2(py)]^{z\,c,e}$	—	2181s	2098s, ≈2060 (sh)	—
$[RuCl_2(CNBu^t)_2(PPh_3)_2]^{z\,f}$	—	2187m	2128s	—
$[RuBr_2(CNBu^t)_2(PPh_3)_2]^{z\,f}$	—	2181m	2124s	—
$[RuCl_3(CNBu^t)_3]^{z\,g}$	—	2238m, 2197s, ≈2160w	—	—
$[RuBr_3(CNBu^t)_3]^{z\,g}$	—	2226m, 2194s, ≈2154w	—	—

[a] Recorded in an IRRAS cell under stated conditions. Relative band intensities: s = strong, m = medium and w = weak. [b] *trans* Isomer. [c] *mer*,*trans* Isomer. [d] Recorded in 0.25 mol dm^{-3} $[NBu_4][PF_6]$ in CH_2Cl_2–MeCN (1 : 1) at ≈290 K. [e] Recorded in 0.5 mol dm^{-3} $[NBu_4][PF_6]$ in CH_2Cl_2–py (1000 : 1) at ≈290 K. [f] *trans*,*trans*,*trans* Isomer. Recorded in 0.5 mol dm^{-3} $[NBu_4][PF_6]$ in CH_2Cl_2 containing 2 mol equivalents of PPh_3 at ≈233 K. [g] *mer* Isomer. Recorded in 0.5 mol dm^{-3} $[NBu_4][PF_6]$ in CH_2Cl_2 containing 5 mol equivalents of $CNBu^t$ at ≈233 K.

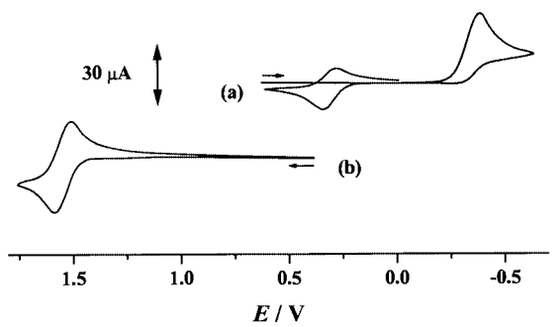

Fig. 2 (a), (b) Cyclic voltammograms of *trans*-$[NBu_4][RuCl_4(CNBu^t)_2]$ in an acetonitrile–dichloromethane (1 : 1) solution containing 0.25 mol dm^{-3} $[NBu_4][PF_6]$ at ≈290 K. Scan rate = 100 mV s^{-1} in each case.

cm^{-1} due to ν_{CN} of co-ordinated acetonitrile confirms the incorporation of a solvent molecule. Oxidation of this product is achieved at $E_{app} = +0.60$ V whereupon ν_{NC} and ν_{CN} move to 2196 and 2328 cm^{-1}, respectively, consistent with the oxidation of Ru^{II} to Ru^{III} (Table 2).

The redox chemistry of these complexes can also be followed by UV-VIS spectroscopy. For ruthenium(III) complexes of general formula $[RuX_nL_{6-n}]^z$ (n = 1–5) the XMCT spectrum can reflect both the number and arrangement of halide ligands about the central metal ion. In certain circumstances mixing can occur between the X^- and L orbitals to perturb this simple model but, for the majority of ligands examined herein, this does not appear to be the case. The VIS spectrum of *trans*-$[RuCl_4(CNBu^t)_2]^-$ [shown in Fig. 3(a)] is similar to that of other *trans* ions $[MCl_4L_2]^-$ (M = Ru or Os),[33–35] with the bands at 487 and 420 nm arising from XMCT transitions of the type $Cl(p\pi) \rightarrow Ru(d\pi)$. Upon reduction of *trans*-$[RuCl_4(CNBu^t)_2]^-$ in acetonitrile in an OTTLE cell, a spectrum with an essentially featureless VIS region is obtained because the possibility of XMCT transitions is eliminated by the filling of the vacancy in the metal $d\pi$ manifold. Upon reoxidation, bands grow at 415, 488 and ≈300 nm, yielding a spectrum indicative of the formation of a tervalent complex containing a meridional arrangement of three chloride ligands,[36–38] *i.e.* *mer*,*trans*-$[RuCl_3(CNBu^t)_2(NCMe)]$. For the analogous bromide complex, the differences between the spectra of *trans*-$[RuBr_4(CNBu^t)_2]^-$ and *mer*,*trans*-$[RuBr_3(CNBu^t)_2(NCMe)]$ are more pronounced on account of the larger spin–orbit coupling constant for the bromide ion.[39]

At temperatures lower than 253 K, the reduction of *trans*-$[RuX_4(CNBu^t)_2]^-$ (X = Cl or Br) in acetonitrile–dichloromethane is chemically reversible on the timescale of the voltammetric experiment (scan rate = 100 mV s^{-1}). However reduction of *trans*-$[RuX_4(CNBu^t)_2]^-$ in the IRRAS cell at low

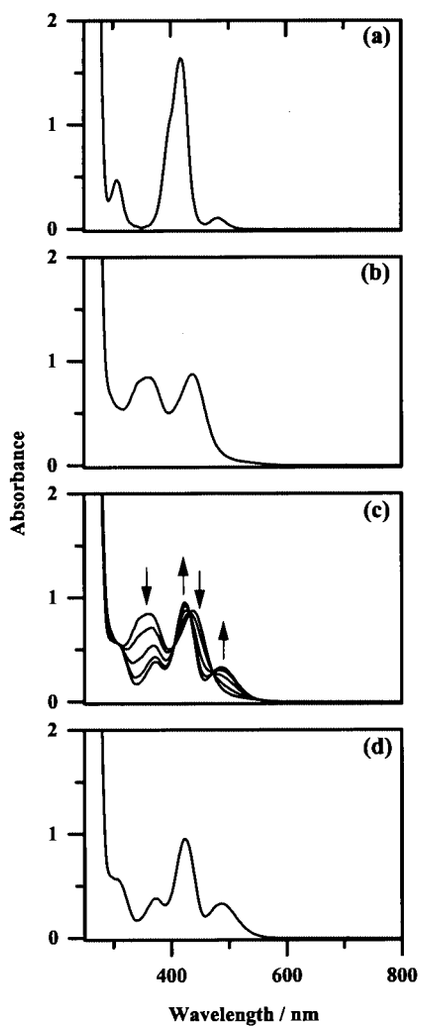

Fig. 3 The UV-VIS spectra of (a) *trans*-$[RuCl_4(CNBu^t)_2]^-$, (b) *mer*, *trans*-$[RuCl_3(CNBu^t)_2(py)]^-$, (c) $[RuCl_3(CNBu^t)_2(py)]^{-/0}$ oxidation, (d) *mer*,*trans*-$[RuCl_3(CNBu^t)_2(py)]$, recorded in an OTTLE cell in pyridine–dichloromethane (1 : 1000) containing 0.25 mol dm^{-3} $[NBu_4][PF_6]$ at 233 K.

temperature proceeds as before, *i.e.* collapse of ν_{NC} from the IR spectrum of the parent complex and growth of ν_{NC} and ν_{CN} due to the formation of *mer*,*trans*-$[RuX_3(CNBu^t)_2(NCMe)]^-$. Although the ions *trans*-$[RuX_4(CNBu^t)_2]^{2-}$ are not sufficiently stable at 233 K to be electrogenerated in their entirety, there is evidence for their formation in the transient growth of ν_{NC} band(s) in the 2050–2100 cm^{-1} region. Once generated, *trans*-

Table 3 UV/VIS Data

Complex (z = charge)	Band maximum[a]/nm (ε/dm^3 mol^{-1} cm^{-1})		
	Ru^{IV}	Ru^{III}	Ru^{II}
$[RuCl_4(CNBu^t)_2]^{z\,b,c}$	≈595 (br) (3100) 528 (5900) 402 (1100) 353 (1300) 283 (5100) 240 (8600)	482 (350) 418 (5100) 302 (1800) 256 (7600)	—
$[RuBr_4(CNBu^t)_2]^{z\,b,d}$	—	656 (300) 566 (5100) 526 (3700) 478 (800) 448 (1300) 366 (1200) 324 (5100)	—
$[RuCl_3(CNBu^t)_2(NCMe)]^{z\,d,e}$	—	488 (4100) 415 (1100) ≈300 (1300)	369 (600)
$[RuBr_3(CNBu^t)_2(NCMe)]^{z\,d,e}$	—	659 (1100) 566 (3300) ≈513 (1600) ≈440 (sh) (600) ≈334 (sh) (1300) 302 (2400)	372 (200)
$[RuCl_3(CNBu^t)_2(py)]^{z\,e,f}$	—	485 (1000) 424 (3000) 371 (1200) ≈300 (1800)	438 (2700) ≈360 (2600)
$[RuBr_3(CNBu^t)_2(py)]^{z\,e,f}$	—	658 (1200) 558 (3600) 438 (1000)	438 (3600) 354 (3200)

[a] Recorded in an OTTLE cell under stated conditions. [b] *trans* Isomer. [c] Recorded in 0.25 mol dm^{-3} $[NBu_4][PF_6]$ in CH_2Cl_2–MeCN (1 : 1) at ≈233 K. [d] Recorded in 0.25 mol dm^{-3} $[NBu_4][PF_6]$ in CH_2Cl_2–MeCN (1 : 1) at ≈290 K. [e] *mer*,*trans* Isomer. [f] Recorded in 0.5 mol dm^{-3} $[NBu_4][PF_6]$ in CH_2Cl_2–py (1000 : 1) at ≈290 K.

$[RuCl_4(CNBu^t)_2]^{2-}$ is less readily substituted by acetonitrile than is the analogous bromide species as judged by the relative lifetimes of their ν_{NC} bands. The voltammetric and spectroscopic details are summarised in Tables 1–3.

Other neutral ligands can similarly be incorporated into the complex at the expense of halide by reduction of dichloromethane–L solutions of *trans*-$[RuX_4(CNBu^t)_2]^-$. In the case of L = py, cyclic voltammetry in dichloromethane–pyridine (1000 : 1) results in the formation of a reversible wave anodically shifted by *ca.* 0.5 V from the $Ru^{III/II}$ couple of the parent complex. The reduction of a dichloromethane–pyridine solution of *trans*-$[RuCl_4(CNBu^t)_2]^-$ in an OTTLE cell ultimately produces the spectrum shown in Fig. 3(b). Attempted reoxidation at $E_{app} = 0.0$ V does not lead to any changes in the UV-VIS spectrum, nor any current flow through the cell, thus confirming that reduction of *trans*-$[RuCl_4(CNBu^t)_2]^-$ results in the formation of *mer*,*trans*-$[RuCl_3(CNBu^t)_2(py)]^-$, a species which is oxidised (or reduced) at a potential different from that of the parent ion. The spectrum of the reduced species [Fig. 3(b)] contains two relatively intense bands at 483 and 363 nm, and differs significantly from that of *mer*,*trans*-$[RuCl_3(CNBu^t)_2(MeCN)]^-$, the spectrum of which is essentially featureless over the VIS region. The difference can be attributed to the coordination of pyridine with its relatively low-lying π* orbital; the bands are thought to arise from metal-to-ligand charge-transfer (MLCT) transitions of the type $Ru(d\pi)\rightarrow py(\pi^*)$.[40,41] At $E_{app} = +0.6$ V oxidative currents are observed and the spectrum shows bands at 485, 424, 371 and ≈300 nm with retention of isosbestic points corresponding to the oxidation of *mer*,*trans*-$[RuCl_3(CNBu^t)_2(py)]^-$ [Fig. 3(c)]. The profile of the final spectrum [Fig. 3(d)] is similar to that of other d^5 *mer*-$[MCl_3L_3]$ complexes[36–38] and the UV-VIS bands are summarised in Table 2. The overall reaction sequence can be summarised by eqns. (1)–(3).

$$\text{E}\quad trans\text{-}[RuX_4(CNR)_2]^- + e^- \rightleftharpoons trans\text{-}[RuX_4(CNR)_2]^{2-} \quad (1)$$

$$\text{C}\quad trans\text{-}[RuX_4(CNR)_2]^{2-} + L \longrightarrow mer,trans\text{-}[RuX_3(CNR)_2L]^- + X^- \quad (2)$$

$$\text{E}\quad mer,trans\text{-}[RuX_3(CNR)_2L]^- \rightleftharpoons mer,trans\text{-}[RuX_3(CNR)_2L] + e^- \quad (3)$$

Reduction of *trans*-$[RuX_4(CNBu^t)_2]^-$ in the presence of a neutral ligand L (PPh_3 or $CNBu^t$)

The end products formed upon reduction of *trans*-$[RuX_4(CNBu^t)_2]^-$ (X = Cl or Br) in the presence of PPh_3 or $CNBu^t$ are different from those described above. For example the reduction of *trans*-$[RuCl_4(CNBu^t)_2]^-$ in an IRRAS cell in 0.25 mol dm^{-3} $[NBu_4][PF_6]$–CH_2Cl_2 containing two equivalents§[42] of PPh_3 results in the formation of a species with a single ν_{NC} band at 2128 cm^{-1}. Reoxidation is not achieved until $E_{app} = +1.00$ V, whereupon ν_{NC} is shifted to 2187 cm^{-1}. The ν_{NC} bands arise from *trans*,*trans*,*trans*-$[RuCl_2(CNBu^t)_2(PPh_3)_2]$ and *trans*,*trans*,*trans*-$[RuCl_2(CNBu^t)_2(PPh_3)_2]^+$ respectively, these species having been prepared and characterised previously.[43] The potential required to achieve oxidation is also consistent with disubstitution, with the $Ru^{III/II}$ couple moving anodically by nearly 1.2 V. In some cases transient monosubstituted species were observed on the timescale of voltammetric experiments, thus indicating that the mechanism for the formation of *trans*,*trans*,*trans*-$[RuX_2(CNBu^t)_2(PPh_3)_2]$ proceeds in a sequential manner through the monosubstituted intermediate. Similarly, the reduction of

§ The use of an excess of PPh_3 prohibits oxidation of the products *trans*,*trans*,*trans*-$[RuX_2(CNBu^t)_2(PPh_3)_2]$, since PPh_3 is oxidised at a lower potential than the complex.

trans-$[RuX_4(CNBu^t)_2]^-$ (X = Cl or Br) in the presence of $CNBu^t$ yields *trans*-$[RuX_2(CNBu^t)_4]$, which can be oxidised reversibly to *trans*-$[RuX_2(CNBu^t)_4]^+$.

The transient nature of *mer*,*trans*-$[RuX_3(CNBu^t)_2(PPh_3)]^-$ and *mer*-$[RuX_3(CNBu^t)_3]^-$ can be attributed to the strong kinetic *trans* effect of the ligands triphenylphosphine and *tert*-butyl isocyanide, labilising the halide in the *trans* position. Limiting the amount of ligand available does not produce different results, only a decrease in the amount of disubstituted product formed. The overall reaction is summarised in eqn. (4).

$$C \quad mer,trans\text{-}[RuX_3(CNR)_2L]^- + L \longrightarrow trans,trans,trans\text{-}[RuX_2(CNR)_2L_2] + X^- \quad (4)$$

Conditions under which *mer*,*trans*-$[RuX_3(CNBu^t)_2(PPh_3)]^-$ and *mer*-$[RuX_3(CNBu^t)_3]^-$ could be stabilised and characterised by *in situ* techniques were not found. In order to characterise the redox chemistry [as given in eqn. (5)] of the products

$$E \quad trans,trans,trans\text{-}[RuX_2(CNR)_2L_2] \rightleftharpoons trans,trans,trans\text{-}[RuX_2(CNR)_2L_2]^+ + e^- \quad (5)$$

trans,*trans*,*trans*-$[RuX_2(CNBu^t)_2(PPh_3)_2]^+$ and *trans*-$[RuX_2(CNBu^t)_4]^+$ more fully, these species have been synthesized, isolated and their electrochemistry examined free from interference of excess of ligand (PPh_3 or $CNBu^t$) and liberated halide X^-.[44]

Oxidation of *trans*-$[RuBr_4(CNBu^t)_2]^-$ in the presence of a neutral ligand L (MeCN, $CNBu^t$ or py)

It has previously been shown that the oxidation of *trans*-$[RuBr_4(CNBu^t)_2]^-$ in 0.25 mol dm^{-3} $[NBu_4][PF_6]$ in acetonitrile–dichloromethane (1 : 1) ultimately leads to the formation of *mer*,*trans*-$[RuBr_3(CNBu^t)_2(NCMe)]$.[19] Similarly, *mer*,*trans*-$[RuBr_3(CNBu^t)_2(py)]$ is formed upon oxidation of *trans*-$[RuBr_4(CNBu^t)_2]^-$ in the presence of pyridine, as summarised in eqns. (6) and (7).

$$E \quad trans\text{-}[RuX_4(CNR)_2]^- \rightleftharpoons trans\text{-}[RuX_4(CNR)_2] + e^- \quad (6)$$

$$C \quad trans\text{-}[RuX_4(CNR)_2] + L \longrightarrow mer,trans\text{-}[RuX_3(CNR)_2L] + {}^1/_2X_2 \quad (7)$$

The oxidative activation of *trans*-$[RuBr_4(CNBu^t)_2]^-$ provides a route to complexes that cannot be prepared *via* the reductive methodology. For instance, it was previously noted that reduction of *trans*-$[RuX_4(CNBu^t)_2]^-$ in the presence of $CNBu^t$ led only to the formation of *trans*-$[RuX_2(CNBu^t)_4]$. The cyclic voltammogram of *trans*-$[RuBr_4(CNBu^t)_2]^-$ in 0.5 mol dm^{-3} $[NBu_4][PF_6]$–dichloromethane containing an excess of $CNBu^t$ reveals an irreversible oxidation at $E_{pa} = +1.50$ V, from which two new species are detected on the return scan at +1.15 and +0.68 V. At low temperature the oxidation of *trans*-$[RuBr_4(CNBu^t)_2]^-$ remains irreversible, although the proportion of that species giving rise to the product wave at +1.15 V is greatly diminished. The IR spectral changes accompanying the oxidation of *trans*-$[RuBr_4(CNBu^t)_2]^-$ in the presence of $CNBu^t$ at room temperature are shown in Fig. 4. Upon oxidation at $E_{app} = +1.6$ V, the ν_{NC} bands from *trans*-$[RuBr_4(CNBu^t)_2]^-$ (2170 cm^{-1}) and free $CNBu^t$ (2139 cm^{-1}) decrease in intensity whilst bands grow at 2226, 2214 and 2195 cm^{-1}. Re-reduction at $E_{app} = +1.0$ V results in the collapse of the band at 2214 cm^{-1} and the growth of another band at 2144 cm^{-1}. Further re-reduction occurs at $E_{app} = +0.5$ V, whereupon the bands at 2226 and 2195 cm^{-1}, and another much less intense band at 2154 cm^{-1}, all decrease in intensity with the growth of a single band at 2144 cm^{-1}. These observations are consistent with the formation of two products upon oxidation of *trans*-$[RuBr_4(CNBu^t)_2]^-$. One of the products is identified as *trans*-$[RuBr_2(CNBu^t)_4]^+$ ($E_{1/2} = +1.15$ V, $\nu_{NC} = 2213$ cm^{-1}). Its identity is also confirmed by the spectral changes observed upon re-reduction at $E_{app} = +1.0$ V. The second product is *mer*-$[RuBr_3(CNBu^t)_3]$ ($E_{1/2} = +0.68$ V). The meridional arrangement of isocyanides in this complex gives rise to three ν_{NC} bands in the IR spectrum, as expected.[45] The bands at 2226 and 2195 cm^{-1} are readily observed but the third band, that at 2154 cm^{-1}, is comparatively weak and is only observed in the difference spectrum for the reduction of *mer*-$[RuBr_3(CNBu^t)_3]$. As discussed previously, *mer*-$[RuBr_3(CNBu^t)_3]^-$ is inherently unstable, rapidly giving way to *trans*-$[RuBr_2(CNBu^t)_4]$ in the presence of additional $CNBu^t$.

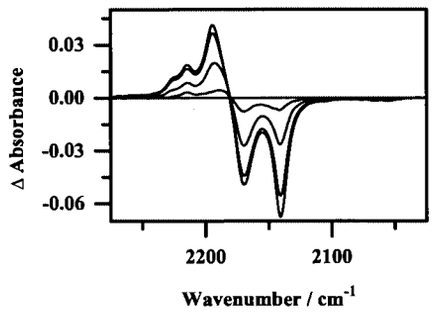

Fig. 4 Changes in the IR difference absorption spectra accompanying oxidation of *trans*-$[NBu_4][RuBr_4(CNBu^t)_2]$ in an IRRAS cell in 0.25 mol dm^{-3} $[NBu_4][PF_6]$–dichloromethane containing free $CNBu^t$. The horizontal line at zero absorbance corresponds to the initial spectrum, *i.e.* that of *trans*-$[RuBr_4(CNBu^t)_2]^-$, prior to electrolysis, ratioed against itself. The potential of the working electrode is stepped to $E_{app} = -0.4$ V, and single scan IR spectra collected as a function of time. Consumption of *trans*-$[RuBr_4(CNBu^t)_2]^-$, upon reduction, is indicated by increasing negative absorbance at 2170 cm^{-1}, whilst increasing negative absorbance at 2139 cm^{-1} corresponds to the change in concentration of free $CNBu^t$. Increasing positive absorbance at 2226 and 2195 cm^{-1} indicates the formation of *mer*-$[RuBr_3(CNBu^t)_3]$ and that at 2214 cm^{-1} the formation of *trans*-$[RuBr_2(CNBu^t)_4]^+$.

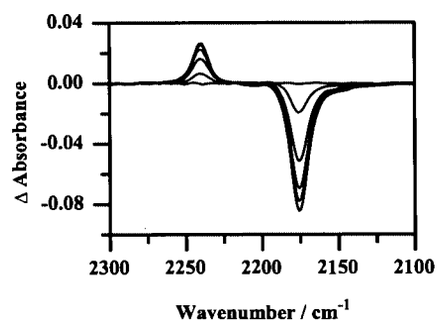

Fig. 5 Changes in the IR difference absorption spectra accompanying oxidation of *trans*-$[NBu_4][RuCl_4(CNBu^t)_2]$ in an IRRAS cell in acetonitrile–dichloromethane (1 : 1) containing 0.25 mol dm^{-3} $[NBu_4][PF_6]$ at 233 K.

Oxidation of *trans*-$[RuCl_4(CNBu^t)_2]^-$

The oxidation of *trans*-$[RuCl_4(CNBu^t)_2]^-$ differs somewhat from that of the analogous bromide complex, in that at low temperature the process is chemically reversible whilst at room temperature multiple products are formed, depending upon the identity of the incoming ligand L.

The cyclic voltammogram of *trans*-$[NBu_4][RuCl_4(CNBu^t)_2]$ in acetonitrile–dichloromethane (1 : 1) containing 0.25 mol dm^{-3} $[NBu_4][PF_6]$ is shown in Fig. 2(b). A quasi-reversible wave is observed at $E_{1/2} = +1.57$ V, indicating that the tetravalent species is stable on the timescale of the voltammetric experiment. Oxidation of *trans*-$[RuCl_4(CNBu^t)_2]^-$ in an IRRAS cell at $E_{app} = +1.70$ V is accompanied by the loss of the parent ν_{NC} band at 2176 cm^{-1}, and simultaneous growth of a single band at 2240 cm^{-1}, as shown in Fig. 5. The single ν_{NC} band indicates

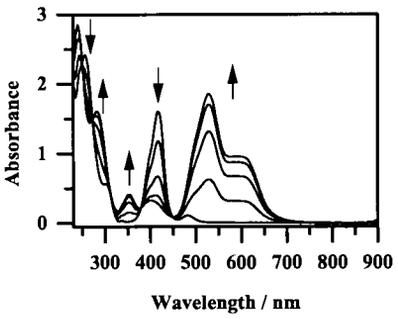

Fig. 6 The UV-VIS spectral changes accompanying oxidation of *trans*-$[NBu_4][RuCl_4(CNBu^t)_2]$ in an OTTLE cell in acetonitrile–dichloromethane (1 : 1) containing 0.25 mol dm^{-3} $[NBu_4][PF_6]$ at 233 K.

retention of the *trans* geometry. At low temperature the spectral changes are fully reversible, in that re-reduction at $E_{app} = +1.40$ V regenerates the starting spectrum, and isosbestic points are observed with each series of spectral changes. The band at 2240 cm^{-1} can be assigned to ν_{NC} of *trans*-$[RuCl_4(CNBu^t)_2]$, which is only the second example of a ruthenium(IV) isocyanide complex.[46] The tetravalent species is evidently quite stable at low temperatures ($T \leq 228$ K), since it is also possible to electrogenerate *trans*-$[RuCl_4(CNBu^t)_2]$ reversibly in an OTTLE cell. The spectral changes accompanying this oxidation of *trans*-$[RuCl_4(CNBu^t)_2]^-$ are shown in Fig. 6. The principal band in the spectrum of *trans*-$[RuCl_4(CNBu^t)_2]^-$ is shifted to lower wavelength (418 to 528 nm) upon oxidation, as anticipated for a XMCT transition of the type $Cl(p\pi) \rightarrow Ru(d\pi)$.[47,48]

The oxidation of *trans*-$[RuCl_4(CNBu^t)_2]^-$ in acetonitrile is considerably more complicated at room than at low temperature. Bulk electrolysis of the chloride at $E_{app} = +1.70$ V gives rise to several species, characterised by reversible waves with $E_{1/2} = +0.33$ and $+0.81$ V and an irreversible wave at $E_{pc} = +0.44$ V. The wave at $+0.33$ V can be attributed to *mer*,*trans*-$[RuCl_3(CNBu^t)_2(NCMe)]$, but the other products remain unidentified at present. The formation of multiple products is confirmed by IR spectroelectrochemical experiments. The mechanism for the oxidative cleavage of a metal–halide bond proceeds *via* a tetravalent intermediate, since *trans*-$[RuCl_4(CNBu^t)_2]$ is identified during the early stage of the electrolysis by its ν_{NC} band at 2240 cm^{-1}, which gives way in time to other bands. The oxidation of *trans*-$[RuCl_4(CNBu^t)_2]^-$ in 0.25 mol dm^{-3} $[NBu_4][PF_6]$ in dichloromethane containing $CNBu^t$ ultimately yields *mer*-$[RuCl_3(CNBu^t)_3]$ and *trans*-$[RuCl_2(CNBu^t)_4]^+$. The relevant data are summarised in Tables 1–3.

Whilst the reductive elimination of halide from complexes of the type $[RuX_nL_{6-n}]^z$ ($n \geq 2$) is well documented,[49–54] *trans*-$[RuX_4(CNBu^t)_2]^-$ are the first of their class to undergo oxidative activation of halide. In some examples of this reaction the cyclic voltammogram clearly shows an X^-/X_2 wave associated with the oxidation of the complex.[55–57] This was not the case for the present system.¶[58,59]

Conclusion

A variety of previously unreported mixed halide–neutral donor ligand complexes have been electrosynthesized from *trans*-$[NBu_4][RuX_4(CNBu^t)_2]$ (X = Cl or Br) and, in most instances, characterised *in situ* by IR and UV-VIS spectroelectrochemistry. The reactions are summarised in eqns. (1)–(7). As has been noted previously, reduction of complexes of this type generally give products in which a halide has been replaced by an available neutral donor ligand. The chloro- and bromo-products are analogous, although there are differences between their stabilities and between the rates at which they are formed. Interestingly cleavage of a metal–halide bond(s) also occurs upon oxidation of these complexes, again resulting in the formation of halide-substituted species. Although for X = Cl it was possible to stabilise the simple one-electron oxidation product at low temperature, complex mixtures of products were always obtained; however in the case of X = Br the reactions proceeded more cleanly. Generally the IR spectroelectrochemical studies have provided considerable insight into the mechanism by which these oxidatively induced reductive-elimination reactions occur.

¶ *In situ* oxidation of a 1 : 2 mixture of *trans*-$[NBu_4][RuBr_4(CNBu^t)_2]$ and the bromide radical spin-trap, $Bu^t(O)NCH–CHN(O)Bu^t$, in an EPR spectroelectrochemical cell produced unidentified radical species. This experiment was complicated by the spin-trap itself undergoing an irreversible two-electron oxidation at $E_{pa} = +1.65$ V.

Acknowledgements

The authors thank Johnson Matthey plc for the loan of hydrated ruthenium trichloride and the Central Research Fund of the University of London for financial assistance. D. G. H. acknowledges the Royal Society for an Endeavour Fellowship and the Ramsay Memorial Fellowships Trust for a British Ramsay Memorial Fellowship. J. P. al D. thanks the EPSRC for a postgraduate award.

References

1 E. A. Seddon and K. R. Seddon, *The Chemistry of Ruthenium*, ed. R. J. H. Clark, Elsevier, Amsterdam, 1984, ch. 8, pp. 155–335.
2 M. Schröder and T. A. Stephenson, *Comprehensive Coordination Chemistry*, ed. G. Wilkinson, Pergamon Press, New York, 1987, vol. 4, pp. 327, 416, 445.
3 X = Cl or Br; L = RCN; C. M. Duff, G. A. Heath and A. C. Willis, *Acta Crystallogr., Sect. C*, 1990, **46**, 2321.
4 X = Cl or Br; L = RCN; S. F. Gheller, G. A. Heath and D. C. R. Hockless, *Acta Crystallogr., Sect. C*, 1995, **51**, 1805.
5 X = Cl; L = Me_2SO; E. Alessio, G. Balducci, M. Calligaris, G. Costa, W. Attia and G. Mestroni, *Inorg. Chem.*, 1991, **30**, 609.
6 X = Cl, Br or I; L = $PhNH_2$; D. L. Key, L. F. Larkworthy and J. E. Salmon, *J. Chem. Soc. A*, 1971, 2583.
7 X = Cl; L = H_2O; D. Rose and G. Wilkinson, *J. Chem. Soc. A*, 1970, 1791.
8 X = Cl; L = PR_3 or AsR_3; T. A. Stephenson, *J. Chem. Soc. A*, 1970, 889.
9 X = Cl; L = imidazole; B. K. Keppler, W. Rupp, U. M. Juhl, H. Endres, R. Niebl and W. Balzer, *Inorg. Chem.*, 1987, **26**, 4366.
10 X = Cl, L = other nitrogen heterocycles; B. K. Keppler, *New J. Chem.*, 1990, **14**, 389.
11 X = Cl, L = py; J. Dehand and J. Rose, *Inorg. Chim. Acta*, 1979, **37**, 249.
12 M. J. Clarke, *Metal Complexes in Cancer Chemotherapy*, ed. B. K. Keppler, VCH, Weinheim, 1993, pp. 129–156.
13 B. K. Keppler, K.-G. Lipponer, B. Stenzel and F. Kratz, *Metal Complexes in Cancer Chemotherapy*, ed. B. K. Keppler, VCH, Weinheim, 1993, pp. 187–220.
14 I. Haiduc and C. Silvestru, *Organometallics in Cancer Chemotherapy*, CRC Press, Boca Raton, 1990, vol. II, pp. 145–151.
15 M. Hartmann, T. J. Einhauser and B. K. Keppler, *Chem. Commun.*, 1996, 1741.
16 M. J. Clarke, *Prog. Clin. Biochem. Med.*, 1989, **10**, 25.
17 M. J. Clarke, *Adv. Chem. Ser.*, 1997, **253**, 351.
18 C. M. Duff and R. A. Schmid, *Inorg. Chem.*, 1991, **30**, 2938.
19 J. P. al Dulaimi, R. J. H. Clark and D. G. Humphrey, *J. Chem. Soc., Dalton Trans.*, 1997, 2535.
20 P. M. Treichel, *Adv. Organomet. Chem.*, 1973, **11**, 21.
21 A. C. Sarapu and R. F. Fenske, *Inorg. Chem.*, 1975, **14**, 247.
22 J. Chatt, C. M. Elson, A. M. Pombeiro, R. L. Richards and G. H. D. Royston, *J. Chem. Soc., Dalton Trans.*, 1978, 165.
23 Y. Yamamoto and H. Yamazaki, *Inorg. Chem.*, 1978, **17**, 3111.
24 W. S. Mialki, D. E. Wigley, T. E. Wood and R. A. Walton, *Inorg. Chem.*, 1982, **21**, 480.
25 T. L. Utz, P. A. Leach, S. J. Geib and N. J. Cooper, *Chem. Commun.*, 1997, 847.
26 C. M. Duff and G. A. Heath, *J. Chem. Soc., Dalton Trans.*, 1991, 2401.

27 I. M. Bell, R. J. H. Clark and D. G. Humphrey, *J. Chem. Soc.*, *Dalton Trans.*, 1999, 1307.
28 R. J. H. Clark and D. G. Humphrey, *Inorg. Chem.*, 1996, **35**, 2053.
29 S. P. Best, S. A. Ciniawsky and D. G. Humphrey, *J. Chem. Soc.*, *Dalton Trans.*, 1996, 2945.
30 S. P. Best, R. J. H. Clark, R. P. Cooney and R. C. S. McQueen, *Rev. Sci. Instrum.*, 1987, **58**, 2071.
31 C. M. Duff and G. A. Heath, *Inorg. Chem.*, 1991, **30**, 2528.
32 P. Pouillen, A. M. Martre and P. Martinet, *Bull. Soc. Chim. Fr.*, 1979, I-387.
33 G. J. Leigh and D. M. P. Mingos, *J. Chem. Soc. A*, 1970, 587.
34 W. Preetz and F. H. Johannsen, *J. Organomet. Chem.*, 1975, **86**, 397.
35 G. A. Heath and D. G. Humphrey, *J. Chem. Soc.*, *Chem. Commun.*, 1991, 1668.
36 A. J. McCaffery and M. D. Rowe, *J. Chem. Soc.*, *Faraday Trans. 2*, 1973, 1767.
37 F. H. Johannsen and W. Preetz, *Z. Anorg. Allg. Chem.*, 1977, **436**, 143.
38 H. Schulz and W. Preetz, *J. Organomet. Chem.*, 1982, **235**, 335.
39 D. H. Whiffen, *Spectroscopy*, Longmans, London, 1966, p. 141.
40 P. Ford, D. F. P. Rudd, R. Gaunder and H. Taube, *J. Am. Chem. Soc.*, 1968, **90**, 1187.
41 A. M. Zwickel and C. Creutz, *Inorg. Chem.*, 1971, **10**, 2395.
42 G. Schiavon, S. Zecchin and G. Cogoni, *J. Electroanal. Chem. Interfacial Electrochem.*, 1973, **48**, 425.
43 Y. Yamamoto, T. Tanase, T. Date, Y. Koide and K. Kobayashi, *J. Organomet. Chem.*, 1990, **386**, 375.
44 D. G. Humphrey, R. J. H. Clark, J. P. al Dulaimi and D. A. Tocher manuscript in preparation.
45 L. J. Lyons, S. L. Pitz and D. C. Boyd, *Inorg. Chem.*, 1995, **34**, 316.
46 M. M. Millar, T. O'Sullivan and N. de Vries, *J. Am. Chem. Soc.*, 1985, **107**, 3714.
47 A. B. P. Lever, *Inorganic Electronic Spectroscopy*, 2nd edn., Elsevier, Amsterdam, 1984, ch. 5, p. 203.
48 B. J. Kennedy and G. A. Heath, *Inorg. Chim. Acta*, 1992, **195**, 101.
49 J. Gulens and J. A. Page, *J. Electroanal. Chem. Interfacial Electrochem.*, 1976, **67**, 215.
50 V. T. Coombe, G. A. Heath, T. A. Stephenson, J. D. Whitelock and L. J. Yellowlees, *J. Chem. Soc.*, *Dalton Trans.*, 1985, 947.
51 J. R. Kirk, D. Page, M. Prazak and V. Katovic, *Inorg. Chem.*, 1988, **27**, 1956.
52 K. J. Taylor and L. J. Yellowlees, *Abstracts 4th Int. Conf. Chemistry of the Platinum Group Metals*, July 1990, C-36.
53 J. A. Corella, R. L. Thompson and N. J. Cooper, *Angew. Chem.*, *Int. Ed. Engl.*, 1992, **31**, 83.
54 D. G. Humphrey, Ph.D. Thesis, The Australian National University, 1992.
55 J. C. Kotz, W. Vining, W. Coco and R. Rosen, *Organometallics*, 1983, **2**, 68.
56 D. R. Tyler, *Prog. Inorg. Chem.*, 1988, **36**, 125.
57 E. Fooladi and M. Tilset, *Inorg. Chem.*, 1997, **36**, 6021.
58 D. G. Humphrey and G. Lazarev, unpublished work.
59 E. G. Janzen, D. Rehorek and H. J. Stronks, *J. Magn. Reson.*, 1984, **56**, 174.

Paper a908241g